

Stellar Image Interpretation System Using Artificial Neural Networks: II – Bi-polar Function Case

A. El-Bassuny Alawy, F. I. Y. Elnagahy, A. A. Haroon, Y. A. Azzam, B. Šimák

A supervised Artificial Neural Network (ANN) based system is being developed employing the Bi-polar function for identifying stellar images in CCD frames. It is based on feed-forward artificial neural networks with error back-propagation learning. It has been coded in C language. The learning process was performed on a 341 input pattern set, while a similar set was used for testing. The present approach has been applied on a CCD frame of the open star cluster M67. The results obtained have been discussed and compared with those derived in our previous work employing the Uni-polar function and by a package known in the astronomical community (DAOPHOT-II). Full agreement was found between the present approach, that of Elnagahy et al, and the standard astronomical data for the cluster. It has been shown that the developed technique resembles that of the Uni-Polar function, possessing a simple, much faster yet reliable approach. Moreover, neither prior knowledge on, nor initial data from, the frame to be analysed is required, as it is for DAOPHOT-II.

Keywords: neural networks, knowledge-based system, stellar images, image processing.

1 Introduction

Not only is stellar astronomy the oldest topic in astronomical studies, but it continues to be of importance in astronomical research. This is because stars are the principle objects from which others are formed (binary and multiple star systems, star clusters and galaxies). Stellar imaging has become an essential and effective technique in astronomy since the invention of photographic plates. Its importance increased with the advent of sophisticated low light level two dimension detectors such as Image Intensifier Tubes (IITs) and Charge Coupled Devices (CCDs).

By the end of the 1970's, astronomical optical observations had made a great leap with the use of cameras equipped with CCD chips after their invention at the Bell Lab. by W. Boyle and G. Smith [1]. This may be attributed to reasons such as superior quantum efficiency, large dynamic and spectral sensitivity ranges, fairly uniform response, high linearity and relatively low noise in comparison with other detectors, particularly photographic plates. In addition, digital image data is directly accessible with no need for measurement or for cumbersome and imprecise calibration. The invention of CCD chips and their use coincided with great advances in of electronic computing machines. As a consequence of these advances, tremendous astronomical images have been acquired that need reliable, precise and fast reduction techniques and approaches.

In the astronomical community various methods have been designed, developed, coded and applied. These are based on viewing the star image through a mathematical model [2, 3, 4], an empirical model [5, 6, 7] or a semi-empirical model [8, 9]. The codes based on these models, usually a bi-variant Gaussian function, require a user-computer interface facility for providing the form of the model adopted and also for setting the initial values of the model parameters. Several runs of such codes are necessary to optimise and derive the final set of parameters, through some non-linear fitting process, to be applicable for CCD frame reduction.

Such circumstances require a fast computing machine provided with a large memory and working space area as well as an expert user. However, incorrect and/or false results are possible, mainly due to imprecise parameter estimates and/or improper user intervention.

Recently, we have developed two approaches employing Artificial Intelligence techniques to recognise stellar images [10] besides deriving all relevant astronomical data [11]. In our previous communication [12], hereinafter Paper I, an Artificial Neural Network based system employing a Unipolar function was proposed. Very good agreement was achieved between the results of our system and those obtained by applying the most widely used software in the astronomical community, DAOPHOT-II [13], through application on a test case (a CCD frame of the star cluster M67). In addition, exact coincidence was found between the results of Paper I and the cluster standard data found in the astronomical literature and databases.

In the present work, a bipolar function has been adopted and applied on the same frame, and the outcome has been investigated and compared with the previous ones.

2 The Problem and the present method

2.1 The problem

As known and outlined in Paper I, a CCD frame may contain entities that are images of astronomical objects (star, galaxy, etc.) as well as those caused by other sources (cosmic rays, noise etc.). All of them are gathered at the same time and under the same atmospheric and instrumental conditions. After acquiring an image, the frame needs to be reduced, first by identifying the stellar images among the others and then by deriving their positions and magnitudes. The present work concerns the first step. This has been realised by a supervised Artificial Neural Network based System (ANNS) as a discriminating approach.

2.2 The architecture of the present ANNS

The ANNS used here is similar to that adopted in Paper I. It comprises the two-layer forward network depicted in Fig. 1. It includes four and three neurones for the first (hidden) layer and the second (output) layer, respectively. The input is z_i (for $i = 1$ to 24) yielding the hidden layer weight matrix as $v(4 \times 24)$ and that of the output as $w(3 \times 4)$. These are illustrated in the figure, which also shows the biases ($v_{1,0}, v_{2,0}, v_{3,0}$ & $v_{4,0}$ and $w_{1,0}, w_{2,0}$ & $w_{3,0}$) for the neurones of the layers. The discriminating function adopted is one of the known bi-polar functions given by the hyperbolic tangent function as

$$F(x) = \frac{1 - e^{-\lambda x}}{1 + e^{-\lambda x}} \quad -1 \leq F(x) \leq 1$$

where λ (descending factor) is an arbitrarily small positive value.

First, the weights for this function have to be determined through the learning process on the selected pattern set. Secondly and before application, both the function adopted and the weights derived have to be verified against a similar known set. Finally, the function and its weights can be applied to an unknown CCD frame to be reduced for the purposes of discrimination.

2.3 Learning and test input patterns

For the learning and test tasks, we adopted the same two pattern sets used in Paper I. In each set, a total of 341 input patterns are included (119 stars, 111 cosmic ray events and 111 noises). It is obvious that the pattern sets are of large size and equally distributed over the three entities. This assures

proper learning and reliable weight determination. For the purpose of learning, the set patterns were randomised and fed to the ANNS. Each pattern consists of the data of a 5×5 pixel array centred at the peaked pixel taken from some CCD frames.

The pattern samples were selected to represent stars of different brightness and events of cosmic rays with different energies as well as various noise patterns. In such a case, the data of the central pixels of the patterns differs widely. In order to perform the learning process properly this data has to be scaled. This was achieved, for each pattern, by normalising the data of all pixels to that of the central pixel. This leads to the unity to all central pixels of the patterns. Fig. 2 demonstrates the raw data, the image and the 3-D view of a sample of these patterns. For the images and 3-D views, normalised data is used. It is evident from the pattern sets, as illustrated in the figure, that:

- a) For a star, the data shows a gradual decrease from the centre outward causing an extended bright area to the limits of the image and a pronounced (but not extreme) sharp peak in the 3-D view.
- b) For a cosmic sample, the central pixel datum is much larger than the data of the other 24 pixels, which is very close to each other with values much lower than those at the centre. This provides very sharp localised peak in the 3-D view and highly concentrated brightness at the centre of the image.
- c) For noise, the data of the array is more or less close to each other and distributed randomly, causing some peaks of low height in the 3-D view, and a featureless image.

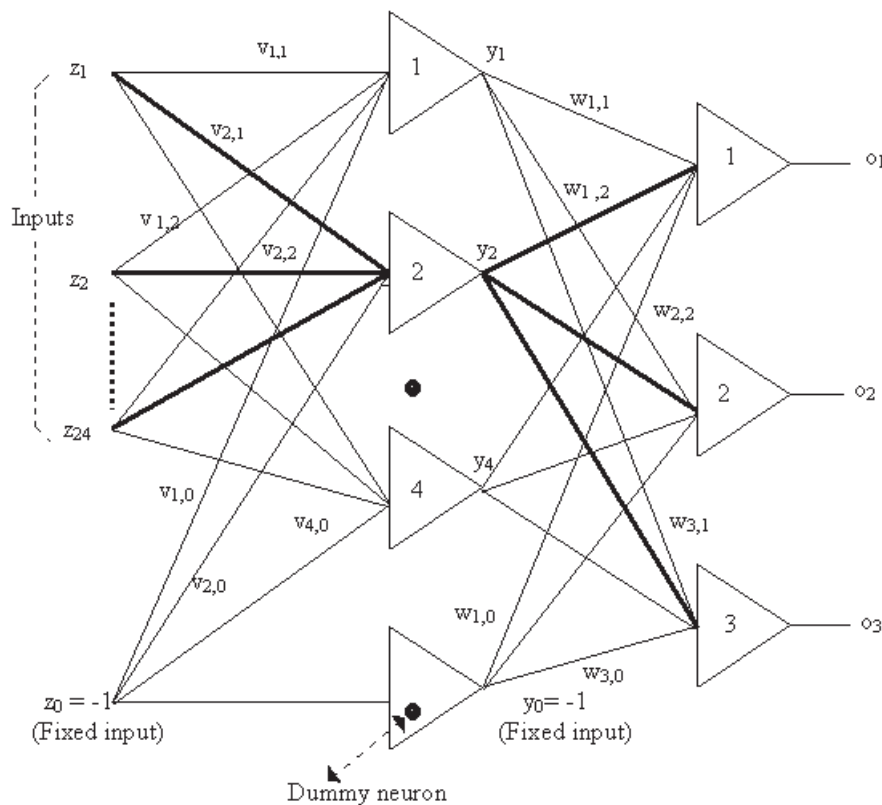


Fig. 1: The architecture of the adopted ANNS

Star					Cosmic event					Noise				
244	505	827	672	219	21	21	22	25	19	20	19	22	25	23
669	1974	3171	1737	406	25	21	25	20	24	23	24	22	22	24
1593	4499	6839	2950	520	22	22	201	85	22	21	21	27	22	21
2091	3825	5474	2256	459	22	19	21	24	23	21	24	25	21	22
1369	1569	1894	941	247	23	22	21	19	24	19	21	24	23	16

Fig. 2: Raw data, image and a 3-D view of a star, cosmic and noise samples of the input pattern

These discriminate characteristics of the three identities are very helpful in applying ANNS.

2.4 Training error and learning factors

The training error and the learning factors adopted here are those described in detail by one of us elsewhere [10] and summarised in [12]. Among the different types of errors workable in ANN, the decision error is invoked to terminate the network training process. It was computed for the entire batch of training pattern samples (P) via,

$$E_d = N_{\text{err}}/PK$$

where K is the threshold output over one cycle (set as 3) and N_{err} is the total number of bit errors resulted.

Regarding the learning mode, some precautions were undertaken for the learning factors in order to avoid the pitfalls generally associated with error minimisation techniques, such as instability, oscillation, divergence and shallow local minima. First, the network weights were initialised randomly to positive values between 0.0 and 0.1, while negative values between these limits were assigned to the biases for the hidden and output layer neurons $v_{i,0}$ and $w_{i,0}$. Secondly, a value of 0.01 was set to the learning constant that was found to accelerate the convergence without overshooting the solution. Finally, the momentum term was set as 0.5 to speed up the convergence of the error back-propagation learning algorithm. The learning factor and the momentum term values are in accordance with the similar values used in Paper I.

2.5 Training the present ANNS

Table 1 lists the desired three components of the output patterns, O_i , nominated for star, noise and cosmic event entities. In the learning mode, many cycles were performed through the adopted patterns. At the beginning of any cycle, N_{err} was set to zero and all input patterns' data were mapped to the ANNS sequentially. For each cycle the first pattern data was fed to the ANNS and the three outputs (i.e. actual output) were computed. For each one of these outputs the error associated was calculated. The total number of bit error (i.e. N_{err}) has to be increased if the difference between the desired output (Table 1) and the actual output is equal to (or greater than) 0.1; then the weights of the output and the hidden layers are adjusted, respectively. Then this process is applied for the next pattern, till the last one providing that the error of each pattern is computed. At the end of the cycle, the decision error (E_d) is computed. If E_d is not equal to zero, the whole cycle is repeated until E_d is zero and hence the learning task is completed.

The decision components of the output patterns, O_i , are given in Table 2 for the three entities (star, noise and cosmic ray event). These are used together with the adopted bi-polar function and the derived weights in order to classify the unknown frame entities. In such a case when Local Central Peaked Pixel (LCPP) is found the 5×5 pixel array data is extracted and the ANNS is employed to compute the relevant outputs and, applying the following:

- If $O_1 > 0.9$, $O_2 < 0.1$ and $O_3 < 0.1$ then the object is a star image.
- If $O_1 < 0.1$, $O_2 > 0.9$ and $O_3 < 0.1$ then the object is a noise.

- If $O_1 < 0.1$, $O_2 < 0.1$ and $O_3 > 0.9$ then the object is a cosmic event.

Table 1: Desired output values for Star, Noise and Cosmic ray event

	O_1	O_2	O_3
Star	1	0	0
Noise	0	1	0
Cosmic Ray	0	0	1

Table 2: Decision output values for Star, Noise and Cosmic ray event

	O_1	O_2	O_3
Star	> 0.9	< 0.1	< 0.1
Noise	< 0.1	> 0.9	< 0.1
Cosmic Ray	< 0.1	< 0.1	> 0.9

2.6 Implementation and test

The present approach was developed to scan the CCD frame to reduce the search for any LCPP whose content is larger than those of the four adjacent pixels at the cardinal directions (see [10, 11]). If such a case is found, the data of the 5×5 pixel array is then normalised with respect to the LCPP datum and mapped to the ANN system. The outputs obtained are compared to the decision output listed in Table 2 to identify the image identity type as star, noise or cosmic ray event within a value of 0.1, which has been adopted as the tolerance limit for learning (Sec. 2.5). The present ANN system has been coded in C language and has been tested through application to the test pattern set (Sec. 2.3). Exact agreement was found between the entities recognised and the prior knowledge on the patterns adopted.

3 Application

After testing the present ANNS, it was applied on a standard CCD frame previously analysed by different methods in order to verify the capability and limitations of the present ANNS in comparison with these methods and the known standard data.

3.1 The case adopted

A CCD frame of the star cluster M67 [14] was undertaken to apply the present ANNS for the following reasons:

- The cluster is one of the standard, well-known and well-studied star clusters, where precise data on the stars in its vicinity is available from several publications and from an accurate database. The region of the cluster imaged in the frame includes faint, intermediate and bright stars, while some stars are close together and some are far apart.
- The frame can be considered as an ideal case for stellar CCD imaging where images of the stars are generally circular. It was obtained together with the widely used software DAOPHOT-II [13] and the relevant and necessary

auxiliary files. Hence reduction of the frame using this code can be achieved properly.

- The frame was reduced by two other approaches through of Knowledge Based System, KBS, [10, 11] and ANNS employing the Uni-polar function [12].

These reasons facilitate an objective comparison of these approaches.

The frame is 320×350 pixels acquired for a period of 30 seconds through the visual optical band where CCD chips have maximum quantum efficiency. The full well capacity value is 16252 ADU (Analog-to-Digital converter Unit).

3.2 Results and discussion

The selected case frame was reduced by applying the present ANNS approach as well as that of Paper I and the DAOPHOT-II code. The last two approaches identify 134 and 137 star images, respectively. A comparison between, and a discussion of, these findings are given in Paper I. The execution of the present technique on the frame showed that:

- The maximum pixel datum is 16252 ADU, where saturation occurred.
- The frame background level is 21.0 (p.e. = ± 1.0).
- Three cosmic events have been identified.
- The frame contains 131 stellar images.

The second finding (i.e. frame background level) is in good agreement with that derived previously as 21.1 [see 11]. The third finding is exactly like that identified by [10, 11]. The computing time is similar to that needed for Paper I, i.e., 45 seconds employing a Pentium II PC (233 MHz Processor) for scanning the image, finding the data limits of the pixels, displaying the frame via the monitor, recognising stellar images and cosmic events and saving the output in the relevant files. During the recognition step, each star image found was marked by an open circle while an open square is displayed around each cosmic event.

In the following, the present results are discussed and compared with those obtained by the other two methods.

3.2.1 The Bi-polar and the Uni-polar function ANNS approaches

Fig. 3 shows the results of applying the two codes. The two approaches agree about identifying the three cosmic events. All stellar images recognised in the present work were identified when the uni-polar function was adopted in Paper I. Three more stellar images were found by applying the latter approach. For these images, it is worthwhile to state that:

- The central pixel data are 33, 35 and 35 (see Table 3). These values are very close to the frame background level (21) and very far from the saturation value (16252). This implies that these are very faint stars having a very low peak-to-background ratio (compare this data with the data in Fig. 2). Hence they are of much less astronomical importance.
- The star discriminator output element O_1 has the values 0.91, 0.92 and 0.94. These values are lower than those of other stars, which are generally larger than 0.99.

Table 3: 5×5 pixel array data for the three very faint stars

Star No. 1					Star No. 2					Star No. 3				
21	19	21	23	24	25	25	29	26	21	21	22	25	24	21
21	27	30	25	21	24	25	29	27	22	21	27	33	26	23
21	28	33	28	25	24	29	35	27	23	23	30	35	28	23
24	27	32	30	18	21	27	28	31	21	24	21	25	21	21
23	22	26	22	21	18	21	22	16	23	22	23	24	23	21

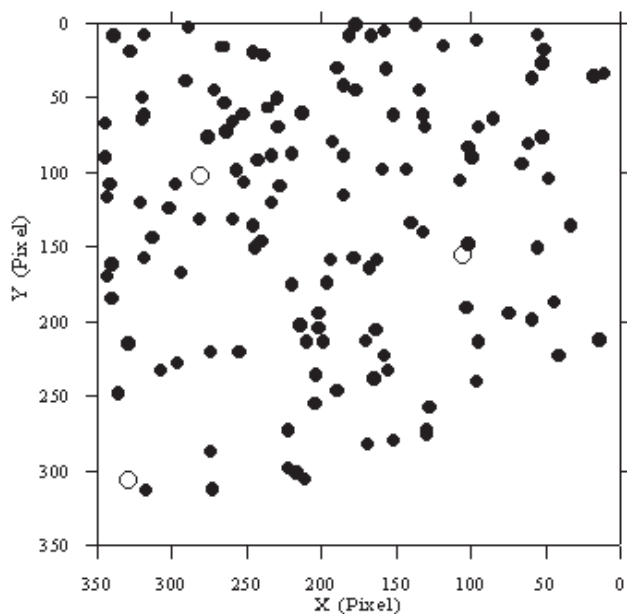


Fig. 3: Map of the images of stars recognised in the M67 star cluster frame (North is up and East to the left). See text.
 Filled circles: images identified by both Uni-polar and Bi-polar functions
 Open circles: images identified by the Uni-polar function only

3.2.2 The Bi-polar function ANNS approach versus the DAOPHOT-II code

As stated above, applying the DAOPHOT-II code on the test case frame leads to recognition of 137 star images; out of these, 131 images were identified by the present approach, showing very good agreement. These common images are displayed in Fig. 4 by filled circles. The remaining six images are shown with different symbols, on which some comments are given. First, three images (denoted by filled squares) are centred at the first or second row (column) close to the frame border. The present approach is not applicable, since no 5×5 pixel array data is available. Nevertheless such locations imply that the stars are partially imaged and hence the images are of no importance from the astronomical point of view. Secondly, two other images (denoted by open circles) are assigned by the DAOPHOT-II code where no images could be found by the present code. At this position, only one very bright star can be seen from the Palomar Observatory Sky Survey (POSS) and the cluster identification charts found in

literature (e.g. [15, 16, 17]). Because of the high brightness of the star the four central pixels are saturated, having the full well capacity value as 16252 (see Table 4a). Another case was found and designated by an open triangle in Fig. 4. In such cases the local area of the frame is treated as two overlapped images by the DAOPHOT-II code, while it is skipped by the present approach because no LCPP is found due to saturation. Finally, the sixth image is at the frame top-left corner and denoted by an open square. On the one hand, one image was identified in the present work. On the other hand the other code assigned two images at almost the same position. According to POSS and the cluster charts, there is one star only in this position. Inspection of the data in the pixels shows that the star image departs slightly from circularity as no radial symmetry around the peaked pixel; the data shows almost two close peaks (see Table 4b). Due to the principles of the present technique, only one LCPP is adopted, leading to one star image. In the DAOPHOT-II code, two overlapped images are considered.

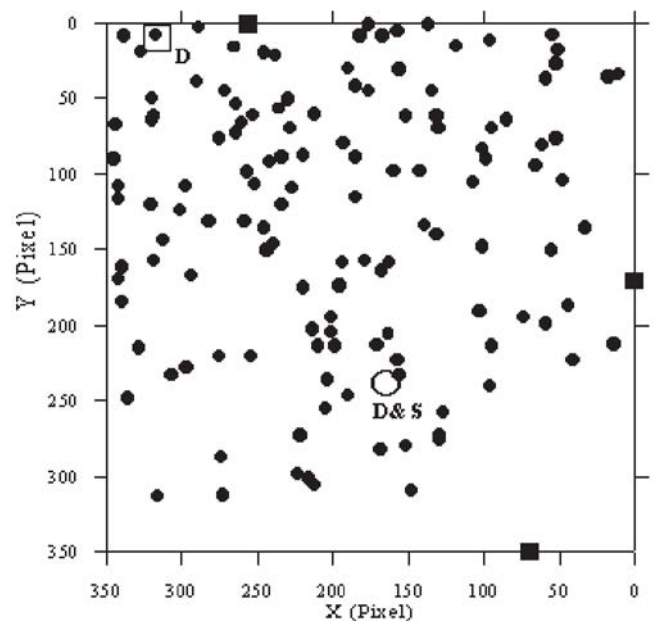


Fig. 4: Map of images of stars recognised in the M67 star cluster frame (North is up and East to the left). See text.
 Filled circles: images identified by Bi-polar function and DAOPHOT-II
 Open circles, square and triangle: images identified by DAOPHOT-II only

Table 4: 8×8 pixel array data for the two stars identified by DAOPHOT-II

a) data for the saturated star image denoted by (D&S) in Fig. 4							
79	124	221	335	429	369	181	93
132	251	624	1386	2108	1175	399	145
198	605	2048	5983	8592	3526	720	219
283	1005	4864	16252	16252	6156	1097	263
295	1065	5534	16252	16252	5659	1005	253
195	623	2437	7443	8213	2985	656	203
121	281	733	1653	1679	844	336	132
83	125	224	365	374	261	137	79
b) data for the deformed star image denoted by (D) in Fig. 4							
25	22	21	26	27	25	25	21
19	24	26	37	38	31	22	22
17	25	38	64	70	47	25	24
25	22	45	97	100	41	25	21
25	23	38	60	67	37	25	21
22	23	31	29	30	27	19	21
22	22	19	25	25	25	24	19
21	20	19	23	24	22	25	21

4 Conclusions

Some conclusions can be drawn from the present study:

Both Uni-polar and Bi-polar functions are good discriminating functions when used in an ANN approach to identify stellar images among the other entities in a CCD frame. Both possess, in comparison with mathematical or empirical star image modelling, the following advantages:

- 1) Extremely short execution time.
- 2) Better and higher recognition ability.
- 3) The two methods do not require complicated non-linear fitting computation, user intervention, prior knowledge or initial values for the star model, a fast computer or large HD free space.
- 4) The ability of the present approach, i.e. display the image and mark the entities found is helpful for visual inspection and for evaluating the outcome of the ANNS technique.
- 5) The results of the Bi-polar function approach agree very well with those obtained in the Uni-polar function case,

except for the images of the three very faint stars. However this may be accounted for by reducing the tolerance value to be less than 0.1 adopted for the training error (Sec. 2.5) in order to enhance the weights of the hidden and output layers.

The two approaches are limited for images centred within the frame up to the third pixel from the frame borders. Any image outside such a region (even if it is a star image) is of no astronomical significance, since it is an incomplete image. Hence this limitation can be ignored.

References

- [1] Boyle W. S., Smith G. E.: "Charge Coupled Semiconductor Devices." *Bell Systems Technical Journal*, Vol. **49** (1970), p. 587–593.
- [2] Blecha R.: "Electronographic Stellar Photometry of Globular Clusters." *Astronomy and Astrophysics*, Vol. **135** (1984), p. 401–409.
- [3] Penny A., Dickens R.: "CCD Photometry of the Globular Cluster NGC6752." *Monthly Notices of the Royal Astronomical Society*, Vol. **220** (1986), p. 845–867.
- [4] Mateo M., Schechter P.: *The DAOPHOT Two-Dimensional Photometry Program*. Proceeding of the first ESO/ST-ECF Data Analysis Workshop, 1989, p. 69.
- [5] Tody D.: "Stellar Photometry in Crowded Fields." *SPIE*, Vol. **264** (1980), p. 171–179.
- [6] Lupton R., Gunn J.: "M13- Main Sequence Photometry and the Mass Function." *Astronomical Journal*, Vol. **91** (1986), p. 317–325.
- [7] Linde P.: *Highlights in Astronomy*. Vol. **8** (1989), p. 651.
- [8] Stetson P.: "DAOPHOT- A Computer Program for Crowded Fields Stellar Photometry." *Publication of the Astronomical Society of the Pacific*, Vol. **99** (1987), p. 191–222.
- [9] Gilliland R., Brown T.: "Time-Resolved CCD Photometry of an Ensemble of Stars." *Publication of the Astronomical Society of the Pacific*, Vol. **100** (1988), p. 754–765.
- [10] Elnagahy F. I. Y.: *MSc Thesis*, Faculty of Engineering, Al-Azhar Univ., Cairo, Egypt, 1988.
- [11] Alawy A. El-Bassuny: "Stellar CCD Photometry: "New Approach, Principles and Application." *Astrophysics and Space Sciences*, Vol. **277** (2001), p. 473–495.
- [12] Elnagahy F. I. Y., Alawy A. E., Simak B., Ella M., Madkour M.: "Stellar Image Interpretation System using Artificial Neural Networks: Uni-polar Function Case." *Acta Polytechnica*, Vol. **41**, No. 6 (2001), p. 33–38.
- [13] Stetson P.: *User's Manual for DAOPHOT-II*. Dominion Astrophysical Observatory, Victoria, Canada, 1996.
- [14] Bojan D.: <http://david.fiz.uni-lj.si/DAOPHOTII>, 1996.
- [15] Eggen O., Sandage A.: "New Photoelectric Observations of Stars in the Old Galactic Cluster M67." *Astrophysical Journal*, Vol. **140** (1964), p. 130–143.
- [16] Johnson H., Sandage A.: "The Galactic Cluster M67 and its Significance for Stellar Evolution." *Astrophysical Journal*, Vol. **121** (1955), p. 616–627.
- [17] Kent A. et al: "CCD Photometry of the Old Open Cluster M67." *Astronomical Journal*, Vol. **106** (1993), p. 181–219.

Assoc. Prof. Ahmed El-Bassuny Alawy
e-mail: abalawy@hotmail.com

Researcher Ali Abdel Wahab Haroon, PhD
e-mail: alyharoon@hotmail.com

Asst. Researcher Eng. Yosry Ahmed Azzam, MSc
e-mail: yosryahmed@hotmail.com

National Research Institute of Astronomy and Geophysics
(NRIAG)
Helwan, Cairo, Egypt

Doc. Ing. Boris Šimák, Csc.
e-mail: simak@feld.cvut.cz

Eng. Farag Ibrahim Younis Elnagahy, MSc
e-mail: faragelnagahy@hotmail.com

Department of Telecommunications Engineering

Czech Technical University in Prague
Faculty of Electrical Engineering
Technická 2
166 27 Praha 6, Czech Republic